Fully Integrated Automotive Radar Sensor With Versatile Resolution

Carsten Metz, *Member, IEEE*, Jens Grubert, Johann Heyen, *Member, IEEE*, Arne F. Jacob, *Member, IEEE*, Stephan Janot, Ernst Lissel, Gerald Oberschmidt, *Member, IEEE*, and Leif C. Stange

***Abstract*—A planar radar sensor for automotive application is presented in this paper. The design comprises a fully integrated transceiver multichip module (MCM) and an electronically steerable microstrip patch array. The antenna feed network is based on a modified Rotman lens. An extended angular coverage, together with an adapted resolution, allows for the integration of automatic cruise control, precrash sensing, and cut-in detection within a single 77-GHz front-end. For ease of manufacturing, the interconnects between antenna and MCM rely on a mixed wire bond and flip-chip approach. The concept is validated by laboratory radar measurements.**

***Index Terms*—Antenna arrays, millimeter-wave radar, MMICs, multichip modules.**

I. Introduction

MILLIMETER-WAVE monolithic integrated-circuit (MMIC) technology and low-profile antennas with high-resolution capability, as well as wide angular coverage, are keys for future low-cost radar systems with high customer acceptance. Due to advanced MMIC production technologies, complete 77-GHz transmit/receive chip sets are readily available for system application [1]–[5]. Here, usually modular approaches are pursued in order to allow maximum flexibility in circuit design. Depending on the desired circuit structure, only a few components like couplers and resonators have to be added. Hence, the engineering tasks focus on the conception of the system architecture including the antenna, design, and optimization of the proper multichip module (MCM), and the chip assembly and characterization. Despite this, most of today's radar front-ends still comprise high-cost packaged Gunn diodes. Present antenna systems mainly rely on quasi-optical concepts or mechanical scanning, which generally implies rather bulky structures [6]–[8]. Only a few reports on planar antennas have been published [9], [10]. Except for increased losses, such concepts are superior with respect to both system integration in the car and low-cost production. Still, additional features like parking aid, precrash sensing, and cut-in detection are presently not integrated in the known 77-GHz antenna designs. Often these tasks are performed by separate 24-GHz modules [11], which complicates the system integration and increases the cost significantly.

Manuscript received March 30, 2001; revised August 22, 2001.

C. Metz is with the Network Hardware Integration Research Department, Bell Laboratories, Murray Hill, NJ 07974 USA.

J. Grubert, J. Heyen, A. F. Jacob, and L. C. Stange are with the Institut für Hochfrequenztechnik, Technical University of Braunschweig, Braunschweig D-38106, Germany.

S. Janot is with Rhode & Schwarz GmbH, Munich 81671, Germany.

E. Lissel is with Volkswagen, 38436 Wolfsburg, Germany.

G. Oberschmidt is with the Information Communication Networks Branch, Siemens, 76646 Bruchsal, Germany.

Publisher Item Identifier S 0018-9480(01)10429-1.

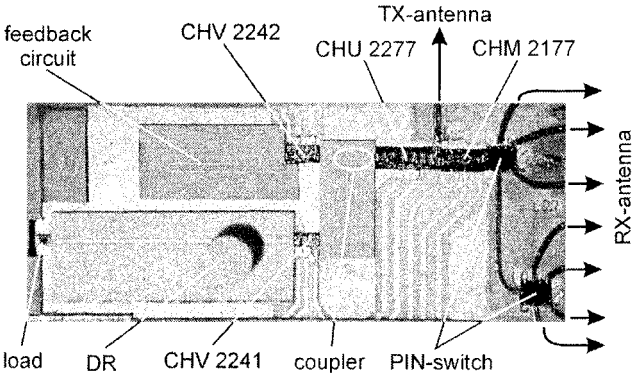

Fig. 1. MCM of the first sensor.

This paper reports on a new planar, fully integrated, and frequency-modulated continuous wave (FMCW) radar sensor for automotive application. Besides a phase-locked loop (PLL) stabilized MMIC chip set, it combines adaptive cruise control (ACC), parking aid, precrash sensing, and cut-in detection capability within a single 77-GHz front-end. To keep the circuit complexity reasonably low, this first prototype system was designed for sequential lobing only. However, parallel lobing can easily be incorporated in future designs because of the flexibility of the present approach. The present planar electronically steerable antenna with its versatile resolution already exhibits the required functionality. Due to the absence of moving parts, the design is rugged and durable. In the following, the transceiver unit and PLL are discussed in detail. Two approaches are presented for both the antenna system and physical structure of the complete front-end. Finally, preliminary operational tests of the overall system are reported.

II. Sensor Hardware Design

A. Transceiver Unit

The assembled MCM is shown in Fig. 1. It consists of 630-μm-thick alumina substrate and incorporates four commercially available MMICs of high functionality [1], two MMIC p-i-n switches [5], and various passive circuit components, designed and manufactured in-house. The gold-plated alumina substrates are structured and shaped employing photolithography and laser material processing, respectively. The MCM is assembled using pick and place utilities with a split-field optic for highly accurate chip placement (± 4 μm). The passive

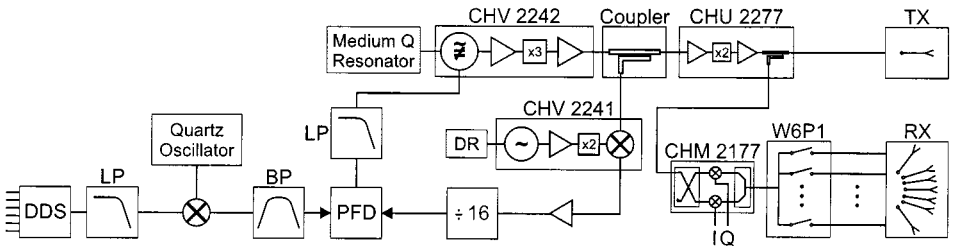

Fig. 2. Block diagram of the sensor.

drop-on components, e.g., an 8-dB microstrip coupler and a medium-Q resonator, were designed on 127-μm-thick alumina substrate, comparable in height to the 100-μm-thick MMIC. All components are connected by wire bonds. The transceiver unit was characterized by means of a Cascade Microtech Probe Station with W-band coplanar-waveguide probes.

Fig. 2 illustrates the architecture of the transceiver unit. A voltage-controlled oscillator (VCO) generates a 12.75-GHz signal, which is amplified and tripled on-chip (CHV2242) to 38.25 GHz. The oscillator is coupled to a medium-Q feedback circuit consisting of three coupled half-wave lines, as suggested in [1]. The oscillator exhibits a free-running phase noise of -75 dBc/Hz@100 kHz and a tuning range exceeding 150 MHz.

The multifunction chip (CHU2277) combines a frequency doubler and a four-stage amplifier. It has two 76.5-GHz ports with an output power of 13 and 9 dBm, respectively. These feed the transmit (TX) antenna and the local-oscillator port of the receiving mixer, respectively.

The integrated in-phase and quadrature (I–Q) mixer (CHM2177) down-converts the signal of the receiving antenna to an in-phase (I) and quadrature (Q) IF port for further signal processing. Sequential lobing of the seven antenna beams is provided by means of p-i-n switch MMIC. Since single-chip 77-GHz SP7T p-i-n switches are currently not available, two W6P1 p-i-n switches [5] had to be cascaded.

In the first prototype, one p-i-n switch MMIC is placed in close proximity to the mixer, whereas the second switch is mounted separately (see Fig. 1). This leads to losses ranging from 6 to 13 dB (10 dB on the average) for the path between antenna and mixer, depending on the connected p-i-n switch.

Fig. 3 shows the design of the MCM used in the second prototype. For more convenient manufacturing the switches are rearranged with respect to the previous design. Due to the optimized signal path and the use of shorter microstrip lines, the losses are now better balanced and reduced by more than 1 dB on the average.

In both configurations, the cascaded p-i-n switch MMIC lead to different power levels for the individual beams. This drawback can be overcome by further optimization of the multiplexer or complete parallel lobing.

B. PLL

In order to suppress VCO phase noise and improve frequency chirp linearity, it is essential to employ phase-lock techniques as a part of the radar synthesizer. An especially demanding requirement for the stepped FMCW approach is the short settling time of 3.5 μs in combination with small frequency steps (approximately 20 kHz) [12]. Typical solutions to this problem include the utilization of multiple-loop architectures or single-loop PLLs with fractional dividers [13].

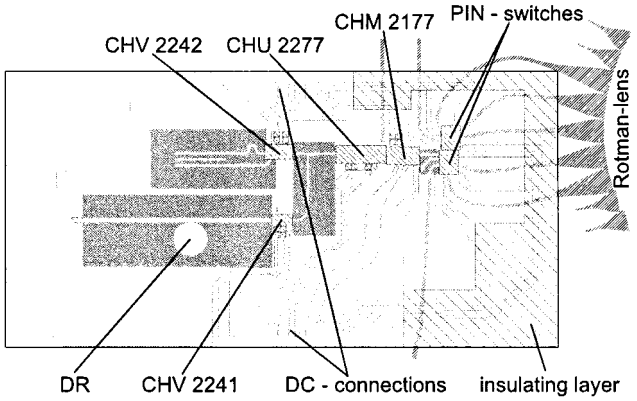

Fig. 3. Layout of the second MCM.

The synthesizer architecture chosen here comprises a single-loop PLL driven by a direct digital synthesizer (DDS) as a reference source. The circuit complexity of this approach is relatively low and enables the selection of standard integrated-circuit (IC) components. DDS exhibit good phase noise performance, fast switching capabilities, and extremely fine frequency resolution. The main problem associated with these devices is their high spurious signal content at higher output frequencies. To alleviate this drawback, the DDS is operated at lower frequencies (4–9 MHz), where the spurious-free dynamic range (SFDR) is sufficiently high, i.e., typically 80 dB within $\pm$100 kHz around the carrier. This output is then up-converted, filtered, and fed to the phase/frequency detector (PFD), as shown in Fig. 2.

The VCO output at 38.25 GHz is partially coupled into the feedback path and down-converted by an integrated oscillator/mixer MMIC (CHV2241). The oscillator is stabilized by means of an external high-Q dielectric resonator (DR) at 19 GHz [1]. Its frequency is doubled internally giving a phase noise of -100 dBc/Hz@100 kHz. The output IF signal in the frequency range of 704–784 MHz is amplified and fed to the PFD through a prescaler/divider chain ($N = 16$) for comparison with the reference signal at 44–49 MHz.

The transmit output spectra are shown in Fig. 4 for the free-running VCO and in Fig. 5 for the phase-locked VCO at 77 GHz. Within 300 kHz around the carrier, the phase noise is efficiently suppressed by typically 10–15 dB, yielding a nominal value of -85 dBc/Hz@100-kHz offset. As can be seen in the plots, spurs at offsets of 500–800 kHz can be suppressed by the PLL to VCO

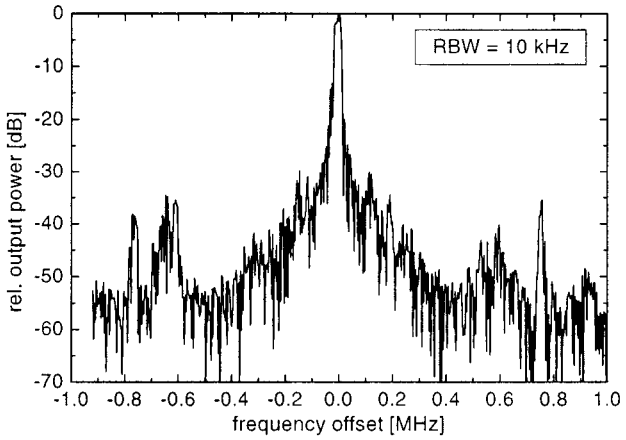

Fig. 4. Spectrum of the transmitted signal with nonstabilized VCO.

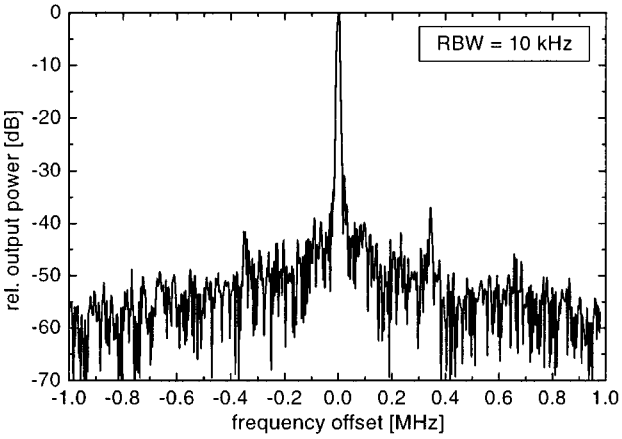

Fig. 5. Spectrum of the transmitted signal due to PLL stabilization of the VCO.

sideband levels. Additional spurs at 350 kHz in the spectrum of the phase-locked oscillator are introduced by the DDS reference, as noted earlier. The transient behavior of the loop, determined by the loop filter bandwidth, is characterized by settling times of less than 1.5 μs.

Only the DR has to be tuned here, making this approach suitable for automatic alignment.

C. Antenna System

The sensor comprises a bistatic antenna system based on a planar microstrip patch array. In the following, receive (RX) and TX antennas will be discussed successively.

For the RX antenna, the required beamwidth is provided by (33×31) elements with 2.7×2.3 mm^2 spacing on a substrate with $\epsilon_r = 3$ and a thickness of 127 μm. The excitation of the array is performed in two stages. First, a Rotman lens sets the phase and amplitude distribution to the 33 columns of the array according to the selected beam (H-plane). The E-plane characteristic (elevation) is determined by 31 series-fed patch rows. This concept is similar to the approach in [9], but with a smaller lens and Fresnel-lens-like designed delay lines. As shown in Fig. 6, the antenna system possesses five beams of 2.7° width at 26.6-dBi average gain (for mechanical reasons, the waveguide measurement equipment could only be connected to four beams in this setup).

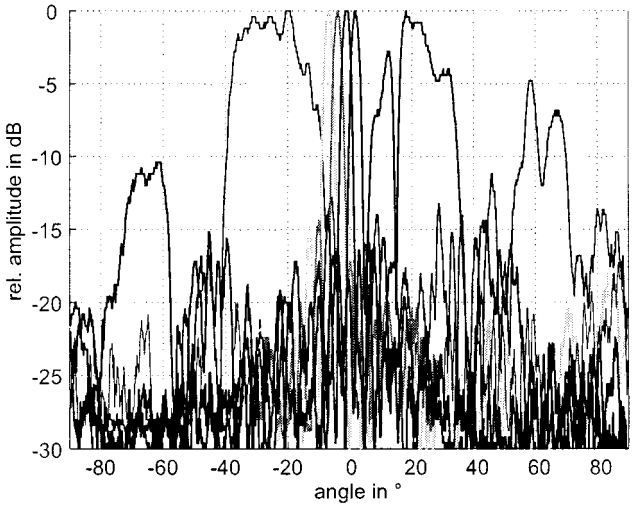

Fig. 6. Measured RX-antenna pattern.

Conventional Rotman lenses are only capable of providing narrow-beam excitation at the array ports. To allow broad-beam generation in azimuth for cut-in detection and precrash sensing capability as well, power splitters are added to the feeding network of the high-resolution ACC antenna, resulting in a distributed feeding of the lens sidewalls. Taking advantage of interference effects within the Rotman-lens parallel-plate waveguide, the distributed excitation is designed so as to emphasize the array center region and to reduce the contribution of the outer array ports. Hence, the latter cannot excite the array and the effective antenna aperture is strongly reduced, which, in the present case, results in a beam broadening of a factor 6.22 and a reduced antenna gain of 16 dB.

In contrast to [9], where TX and RX antenna were scanned simultaneously, here, the entire field of view is illuminated permanently. The TX antenna consists of 4×31 elements and a passive power splitter. Due to the wider angular coverage, only four columns of the array have to be utilized for the azimuth.

To provide an adapted irradiation, the long-range domain is illuminated with the main lobe, while the short-range domains are supplied with much less power via the 12.5-dB lower sidelobes of the antenna pattern. To prevent zeros in the radiation diagram, a nonequidistant element spacing is applied (here, 2.24, 2.34, and 2.24 mm) to ensure a smooth transition between the main-lobe and first sidelobe region. With a half-power beamwidth of 22°, the resulting radiation pattern, shown in Fig. 7, exhibits a gain of 23 dB and covers the required azimuthal angular range entirely.

As mentioned before, the 31 series-fed patch rows determine the E-plane characteristic. Here, the element spacing is chosen to yield a phase separation between the antenna elements of exactly 2π. Thus, all elements work in-phase so that the main lobe is at broadside. Two designs with different feeding points were investigated.

In a first approach, the patch columns were fed at their endpoints, leading to overall dimension of the antenna system of 10-cm width $\times$ 23-cm length. Fig. 8 shows the corresponding simulated and measured antenna pattern. The latter is misaligned by 1.8° compared to the simulated characteristic.

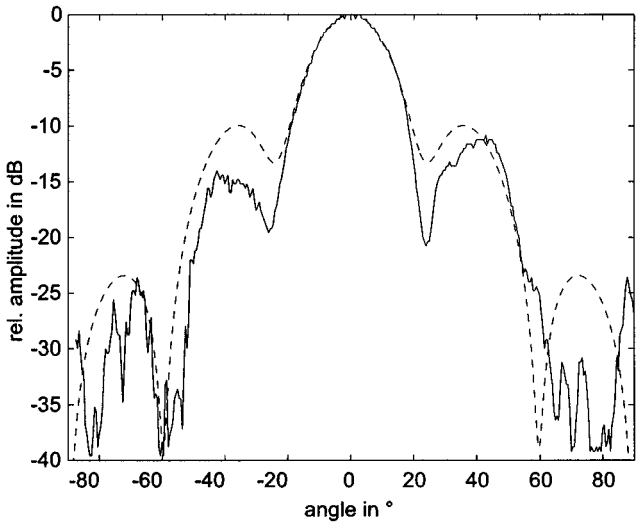

Fig. 7. Measured antenna characteristic (azimuth) of the TX antenna.

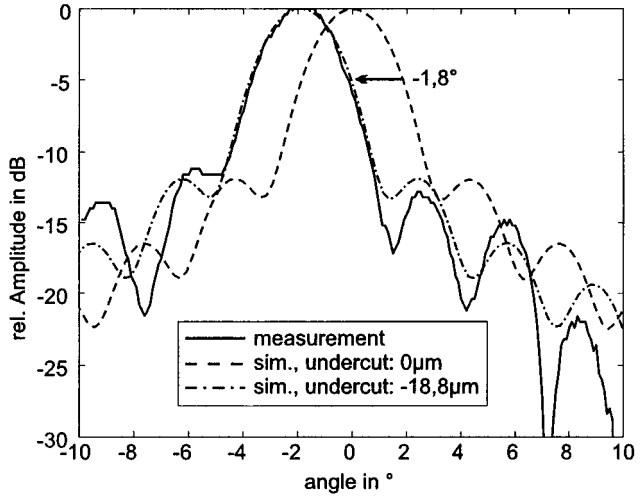

Fig. 8. Measured elevation pattern.

This is due to the fact that the asymmetrical excitation is prone to phase errors. Simulations confirm that these mainly originate from defects in the manufacturing process. Here, the misalignment of the main lobe can be attributed to a deviation of the linewidth of 38 μm.

In a second approach, the patch columns were fed at their center element to overcome the deviation of the main lobe in the E-plane due to asymmetric phase errors.

In this case, the feeding was realized by aperture coupling. The antenna then consists of two dielectric and three metal layers. The patch array resides on top of the multilayer substrate, while the feed network consisting of a Rotman lens is located on the bottom side. A common ground plane between the two dielectric layers provides coupling slots to excite the array and prevents spurious radiation from the feed network. Besides better performance, this approach offers a size reduction of 3.5 cm in length compared to the series-fed configuration, where the Rotman lens and patch array are placed on one substrate.

Systematic studies show that the influence of the slot radiation on the antenna diagram can be minimized by placing the slot under the center patch. The feed line is matched by means of an open-ended stub configuration.

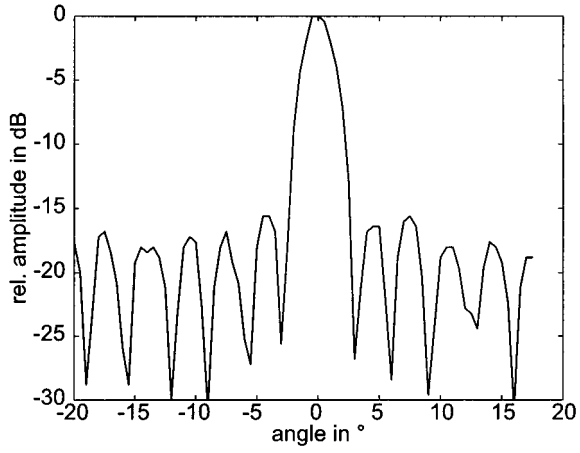

Fig. 9. Measured elevation pattern of center-fed antenna system.

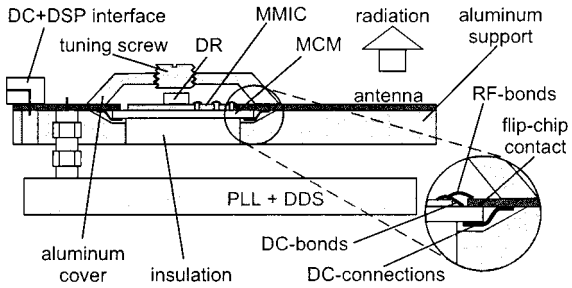

Fig. 10. Physical structure of the first front-end.

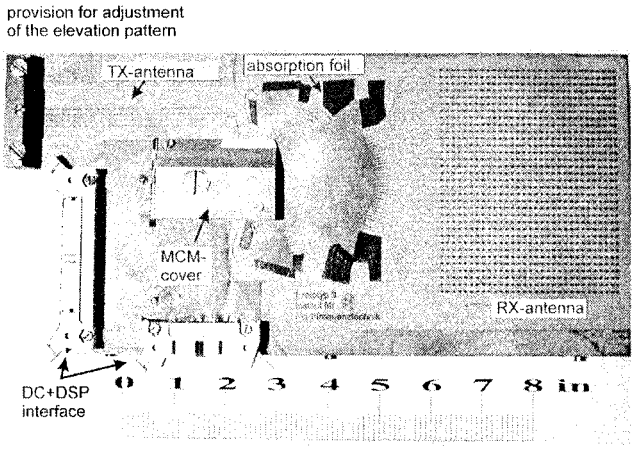

Fig. 11. Planar sensor.

Furthermore, the manufacturing process for highly accurate alignment and bonding of the two substrates was optimized experimentally. Positioning marks were placed on both the substrates and photo masks. Additional optical monitoring during the assembly of the antenna permitted a placement reproducibility of better than 10 μm. The bonding was performed using nonconductive two-component epoxies at low temperature and low pressure in order to reduce the stress on the microstrip circuitry on the soft substrate.

Fig. 9 shows the measured E-plane characteristic of a center-fed antenna array in multilayer technology. The main

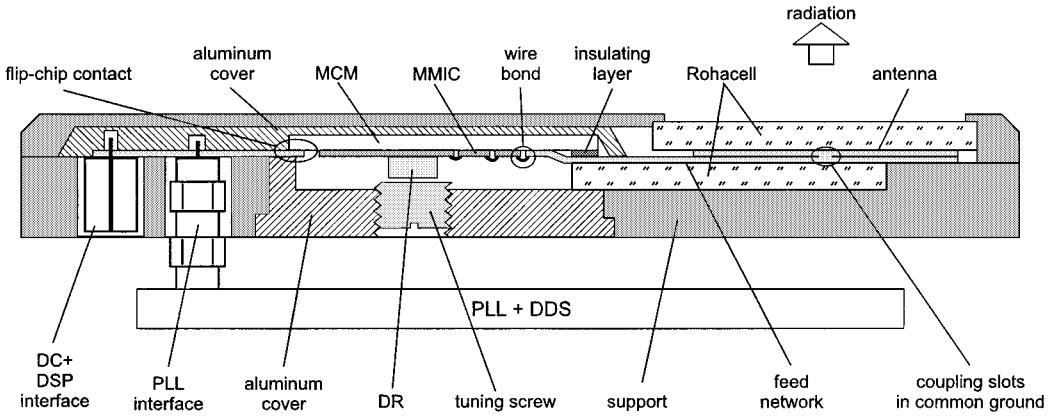

Fig. 12. Physical structure of the second front-end with radome.

lobe is located exactly at broadside and the first sidelobes are reduced by 4 dB compared to the series-fed configuration. The improved sidelobe level results from the symmetric feeding of the array, which causes the current distribution on the patches to fall off exponentially to both ends of the patch column.

D. Physical Structure of the Front-End

While all RF connections are wire bonded, the dc and IF interconnects between the MCM and antenna substrate are flip-chipped using conductive adhesives. To minimize the bond length and, thus, transmission losses, the antenna substrate and MMIC have comparable thickness. In the first prototype, the conducting traces of the dc supply are partly configured on the backside of the MCM to avoid intersections of RF and dc. Fig. 10 shows a cross-sectional view of the first prototype front-end. The insert details the dc transition between the MCM topside, the backside of the soft substrate, and the MCM backside. An aluminum plate supports the antenna substrate and MCM. A radome was omitted in the laboratory prototype shown in Fig. 11.

In the second design, for ease of manufacturing, all dc traces are located on the top side of the MCM, which is mounted upside down. A thin insulating layer now needs to be inserted between the MCM and antenna substrate. This configuration is illustrated in Fig. 12. The feed network is supported by a layer of Rohacell to avoid impairment of its electrical characteristics due to package influence. Another Rohacell layer serves as a radome for the antenna. The transverse dimensions of the support are 23 cm $\times$ 12 cm, its thickness being 2.2 cm. The PLL adds another 4 cm, currently still leaving great potential for miniaturization.

III. Results

Functionality tests of the first prototype (Figs. 10 and 11) were conducted in a laboratory environment. The digital signal processing (DSP) was run on a standard personal computer (PC). This includes all necessary FMCW-waveform settings for the DDS and data acquisition. The measurements are performed as follows. Before down-conversion, the received RF signal is chopped by a 20-kHz "on–off-keying" of the MMIC switches in the receiving path. The modulated baseband signal is measured with a commercial lock-in-amplifier (Stanford Research Systems SR-510), which is synchronized to the chopper signal. The measured data are transferred to the PC for further signal processing, which allows online radar measurements of stationary targets. Since the PC interfaces used are too slow, Doppler processing is not feasible in this test setup. For illustration, Fig. 13 shows the processed signal obtained from a corner reflector located at 18 and 23 m, respectively. An appropriate DSP architecture will now be added to the front-end in order to allow velocity measurements. Its improved offset correction will increase the sensitivity. Further work is currently devoted to the realization and functionality tests of the second front-end (Fig. 12).

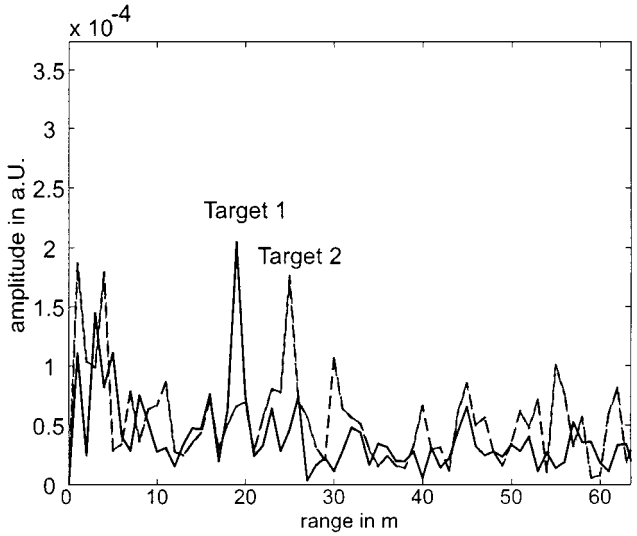

Fig. 13. Radar measurements with targets at 18 and 23 m.

IV. Conclusion

In this paper, two configurations of a fully integrated planar radar sensor for automotive application have been presented. ACC, precrash sensing, and cut-in detection have been integrated within one 77-GHz front-end to replace today's hybrid approaches based on separate 24- and 77-GHz modules. Commercially available MMIC and self-made components have been employed for the transceive module. A detailed description of the technological fabrication process has been given. The electrical interface between the antenna and MCM

has been realized in mixed flip-chip and wire-bond technology to reduce the number of bond wires. For phase noise reduction, the oscillator has been stabilized by a PLL. Simple radar measurements have proven the functionality. A DSP unit is now being attached to the front-end for high-performance detection and field application.

ACKNOWLEDGMENT

The authors wish to acknowledge the continuous and generous support of both United Monolithic Semiconductors (UMS) and Tyco Electronics M/A-COM regarding the supply of the MMICs.

REFERENCES

[1] M. Camiade, D. Domnesque, Z. Quarch, and A. Sion, "Fully MMIC-based front end for FMCW automotive radar at 77 GHz," in *Proc. Eur. Microwave Conf.*, vol. 1, Paris, France, 2000, pp. 9–12.

[2] H. J. Siweris, A. Werthof, H. Tischer, U. Schaper, A. Schafer, L. Verweyen, T. Grave, G. Bock, M. Schlechtweg, and W. Kellner, "Low-cost GaAs pHEMT MMIC's for millimeter-wave sensor applications," *IEEE Trans. Microwave Theory Tech.*, vol. 46, pp. 2560–2567, Dec. 1998.

[3] H. Mizutani, N. Shida, T. Saryo, T. Kuwabara, T. Eda, T. Matsumura, and M. Funabashi, "76-GHz MMIC chip set for compact, low cost and highly reliable automotive radar system," in *IEEE Radio Freq. Integrated Circuits Symp. Dig.*, 1999, pp. 91–94.

[4] H. Kondoh, K. Sekine, S. Takatani, K. Takano, H. Kuroda, and R. Dabkowski, "77 GHz fully-MMIC automotive forward-looking radar [using pHEMTs]," in *21st Annu. GaAs IC Symp.*, 1999, pp. 211–214.

[5] J. Putnam, M. Barter, K. Wood, and J. LeBlanc, "A monolithic GaAs PIN switch network for a 77 GHz automotive collision warning radar," in *IEEE MTT-S Int. Microwave Symp. Dig.*, vol. 2, 1997, pp. 753–756.

[6] L. H. Eriksson and B.-O. As, "Autmotive radar for adaptive cruise control and collisions warning/avoidance," in *Radar'97*, Järfälla, Sweden, pp. 16–20.

[7] W. Menzel, D. Pilz, and R. Leberer, "A 77-GHz FM–CW radar front-end with a low-profile low-loss printed antenna," *IEEE Trans. Microwave Theory Tech.*, vol. 47, pp. 2237–2241, Dec. 1999.

[8] K. Winter, B. Lucas, H. Olbrich, T. Beez, H. Mayer, and K. Lehre, "A compact radar sensor and control unit for adaptive cruise control," in *Int. Radar Symp. Dig.*, vol. 1, Munich, Germany, 1998, pp. 355–362.

[9] M. E. Russell, A. Crain, A. Curran, R. A. Campbell, C. A. Drubin, and W. F. Miccioli, "Millimeter-wave radar sensor for automotive intelligent cruise control," *IEEE Trans. Microwave Theory Tech.*, vol. 45, pp. 2444–2453, Dec. 1997.

[10] D. D. Li, S. C. Luo, and R. M. Knox, "Millimeter-wave FMCW radar transceiver/antenna for automotive applications," *Appl. Microwave Wireless*, vol. 11, no. 6, pp. 58–68, 1999.

[11] P. Heide, M. Vossiek, M. Nalezinski, L. Oréans, R. Schubert, and M. Kunert, "24 GHz short-range microwave sensors for industrial and vehicular applications," in *Short Range Radar Workshop*, Ilmenau, Germany, 1994.

[12] R. Mende and H. Rohling, "A high performance AICC radar sensor-concept and results with an experimental vehicle," in *Radar'97*, Järfälla, Sweden, pp. 21–25.

[13] T. v. Kerssenbrock, T. Musch, B. Schiek, and P. Heide, "Novel 77 GHz low-cost automotive radar module with fractional-PLL frequency linearizer," in *Proc. Eur. Microwave Conf.*, Munich, Germany, 1999, pp. 5–8.

Carsten Metz (M'98) was born in Göttingen, Germany, in 1972. He graduated from the Technical University of Braunschweig, Braunschweig, Germany, in 1997, and received the Dr.-Ing. degree in automotive radar sensors with versatile resolution from the Technical University, Braunschweig, Germany, in 2001.

He is currently with the Network Hardware Integration Research Department, Lucent Technologies, Bell Laboratories, Murray Hill, NJ. His research interests include digital beamforming, antenna designs, and multilayer approaches for MCM packaging.

Jens Grubert was born in Wolfsburg, Germany, in 1973. He received the Dipl.-Ing. degree in electrical engineering from the Technical University of Braunschweig, Braunschweig, Germany, in 1999.

He is currently with the Institut für Hochfrequenztechnik, Technical University of Braunschweig. His research interests include design and characterization of multichip circuits and interconnects at millimeter waves and propagation measurements at microwave.

Johann Heyen (M'99) was born in Aurich, Germany, in 1973. He received the Dipl.-Ing. degree in electrical engineering from the Technical University of Braunschweig, Braunschweig, Germany, in 1999, and the M.S.E.E. degree from the University of Rhode Island, Kingston, in 1999, and is currently working toward the Ph.D. degree in millimeter-wave applications and techniques at the Technical University of Braunschweig.

Since 1999, he has been with the Microwave Technology Group, Institut für Hochfrequenztechnik, Braunschweig, Germany. His research interests include multilayer approaches for MCM packaging and antenna designs.

Arne F. Jacob (S'79–M'81) was born in Braunschweig, Germany, in 1954.

He received the Dipl.-Ing. and Dr.-Ing. degrees from the Technical University of Braunschweig, Braunschweig, Germany, in 1979 and 1986, respectively.

From February 1986 to January 1988, he was a Fellow at the European Laboratory for Particle Physics, CERN, Geneva, Switzerland. From February 1988 to September 1990, he was with the Accelerator and Fusion Research Division, Lawrence Berkeley Laboratory, University of California at Berkeley. Since 1990, he has been a Professor at the Institut für Hochfrequenztechnik, Technical University of Braunschweig. His current research interests include the design and application of planar circuits at microwave and millimeter frequencies, and the characterization of complex materials.

Stephan Janot was born in Halle (Saale), Germany, in 1972. He received the Dipl.-Ing. degree from the Technical University of Braunschweig, Braunschweig, Germany, in 2000.

In 1994, he completed his vocational training as an Electrician. He is currently involved with electronic projects dealing with synthesizers and microwave receiver front ends at Rhode & Schwarz GmbH, Munich, Germany.

Ernst Lissel was born in Poischwitz/Schlesien, Germany, in 1941. He received the Dipl.-Ing. degree in RF and communication electronics from the Technical University of Hanover, Hanover, Germany, in 1966.

He developed test equipment for telecommunication links prior to joining Volkswagen (VW), Wolfsburg, Germany, in 1970. With Volkswagen, he has been involved in various vehicle electronic projects dealing with body control, brake control, sensors, and automotive radar applications. In the PROMETHEUS Program, he represented VW in the Adaptive Cruise Control (ACC) Working Group. As a Senior Engineer in the VW Research Department, he was responsible for advanced automotive radars and active safety projects using radar technology.

Gerald Oberschmidt (M'94) received the Master of Science degree in electrical engineering from the Georgia Institute of Technology, Atlanta, GA, in 1993. He graduated from the Technical University of Braunschweig, Braunschweig, Germany, in 1994, and received the Dr.-Ing. degree on wavelet-based simulation of microwave planar circuits from the Technical University of Braunschweig in 1999.

He is currently with the Information Communication Networks Branch, Siemens, Bruchsal, Germany, where he is involved with third-generation mobile radio systems.

Dr. Oberschmidt was the recipient of the Heinrich Büussing Award for the 2001 outstanding dissertation of the Technical University Braunschweig.

Leif C. Stange was born in Hamburg, Germany, in 1974. He received the Dipl.-Ing. degree from the Technical University of Braunschweig, Braunschweig, Germany, in 2000.

He is currently an Assistant Research Engineer with the Institut für Hochfrequenztechnik, Technical University of Braunschweig. His research activities focus on active antenna arrays for radar and satellite communications.